Self-consistent implementation of a nonlocal van der Waals density functional with a Gaussian basis set

Oleg A. Vydrov, Qin Wu, and Troy Van Voorhis

Citation: J. Chem. Phys. **129**, 014106 (2008); doi: 10.1063/1.2948400
View online: http://dx.doi.org/10.1063/1.2948400
View Table of Contents: http://jcp.aip.org/resource/1/JCPSA6/v129/i1
Published by the AIP Publishing LLC.

Self-consistent implementation of a nonlocal van der Waals density functional with a Gaussian basis set

Oleg A. Vydrov,[a] Qin Wu, and Troy Van Voorhis
Department of Chemistry, Massachusetts Institute of Technology, Cambridge, Massachusetts 02139, USA

(Received 16 April 2008; accepted 28 May 2008; published online 3 July 2008)

Nearly all common density functional approximations fail to properly describe dispersion interactions responsible for binding in van der Waals complexes. Empirical corrections can fix some of the failures but cannot fully grasp the complex physics and may not be reliable for systems dissimilar to the fitting set. In contrast, the recently proposed nonlocal van der Waals density functional (vdW-DF) was derived from first principles, describes dispersion interactions in a seamless fashion, and yields the correct asymptotics. Implementation of this functional is somewhat cumbersome: Nonlocal dependence on the electron density requires numerical double integration over the space variables and functional derivatives are nontrivial. This paper shows how vdW-DF can be implemented self-consistently with Gaussian basis functions. The gradients of the energy with respect to nuclear displacements have also been derived and coded, enabling efficient geometry optimizations. We test the vdW-DF correlation functional in combination with several exchange approximations. We also study the sensitivity of the method to the basis set size and to the quality of the numerical quadrature grid. For weakly interacting systems, acceptable accuracy in semilocal exchange is achieved only with fine grids, whereas for nonlocal vdW-DF correlation even rather coarse grids are sufficient. The current version of vdW-DF is not well suited for pairing with Hartree–Fock exchange, leading to considerable overbinding. © *2008 American Institute of Physics*. [DOI: 10.1063/1.2948400]

I. INTRODUCTION

van der Waals (vdW) interactions are crucial for the chemistry and physics of weakly bound systems,[1] such as biological macromolecules, layered materials, organic crystals, molecules adsorbed on surfaces, etc. A computational tool aspiring to give useful predictions for such systems must properly account for vdW forces. Density functional theory (DFT) appears to be the most popular electronic structure method nowadays. Unfortunately, the vast majority of commonly used DFT approximations fail to properly describe dispersion interactions. vdW potentials predicted by common functionals can be either repulsive or attractive at short range but always fail to reproduce the correct asymptotics. It can further be argued that attractive interactions produced by some local and semilocal functionals arise for the wrong reasons: The binding comes entirely from the density overlap region and therefore scales incorrectly with the system size.[2] Such attractive interactions usually originate from a (semi)local exchange component, whereas in reality the dispersion interaction, responsible for vdW attractive forces, is a nonlocal correlation effect.

Recently a number of semiempirical corrections have been proposed to amend common approximate functionals. One popular scheme[3–6] consists in adding a force-field-like pairwise potential where interaction between each pair of atoms is approximated by a damped multipole expansion, often (but not always) truncated after the first term C_6/R^6. Apart from a number of simplifications, such as the assumption of pairwise additivity of vdW forces, the presence of empirically fitted parameters in such methods can lead to unreliable results for systems dissimilar to the training set. There exist more rigorous specialized DFT-based methods for estimating dispersion interactions.[7–11] However, many of these techniques require separation of a system into clearly defined interacting fragments and hence cannot be easily applied to intramolecular interactions. We choose not to give a detailed review of vdW approximations in DFT but refer an interested reader to reviews and comparisons compiled elsewhere.[12,13]

In contrast to the majority of approximations, the nonlocal van der Waals density functional (vdW-DF) proposed in Ref. 14 was derived from first principles, describes dispersion interactions in the most general and seamless fashion, and yields the correct asymptotics. vdW-DF has been successfully applied to weakly bound molecular complexes,[14–18] polymer crystals,[19] and molecules adsorbed on surfaces.[20,21] A more widespread use of this promising functional seems to be somewhat hindered by the fact that its implementation is nontrivial, especially when self-consistency is desired. A self-consistent implementation within a plane-wave code has been reported only very recently.[17] Note that all calculations with vdW-DF reported to date have been non-self-consistent with the sole exception of Ref. 17. Self-consistency and analytic gradients are required for standard molecular structure optimization techniques. Reference 17 reports the only gradient-based geometry optimization with vdW-DF so far.

In this paper, we present a robust self-consistent imple-

[a]Electronic mail: vydrov@mit.edu.

mentation of vdW-DF with Gaussian basis functions. We also derive and test the gradients of the energy with respect to nuclear displacements, which enable us to perform geometry optimizations efficiently. We test the vdW-DF correlation functional in combination with several exchange components and also study the effects of the basis set size as well as the effects of the fineness of the numerical quadrature grid. We identify a few issues, mostly technical in nature, that are yet to be resolved.

II. METHODOLOGY AND IMPLEMENTATION

The total correlation (c) energy in vdW-DF is defined[14] as a sum of the correlation energy in the local density approximation (LDA) and a fully nonlocal (nl) part,

$$E_c^{\text{vdW-DF}} = E_c^{\text{LDA}} + E_c^{\text{nl}}. \tag{1}$$

We use the functional of Vosko *et al.*[22] for E_c^{LDA} (parametrization 5, also known as VWN5). The nl term in Eq. (1) is written as

$$E_c^{\text{nl}} = \frac{1}{2}\int d\mathbf{r}\rho(\mathbf{r})\int d\mathbf{r}'\rho(\mathbf{r}')\phi(\mathbf{r},\mathbf{r}'). \tag{2}$$

The kernel ϕ is more conveniently expressed[14] in terms of the variables d and d',

$$d(\mathbf{r},\mathbf{r}') = |\mathbf{r}-\mathbf{r}'|q_0(\mathbf{r}), \tag{3}$$

$$d'(\mathbf{r},\mathbf{r}') = |\mathbf{r}-\mathbf{r}'|q_0(\mathbf{r}'), \tag{4}$$

with

$$q_0(\mathbf{r}) = -\frac{4\pi}{3}(\varepsilon_c^{\text{LDA}}(\mathbf{r}) + \varepsilon_x^{\text{LDA}}(\mathbf{r})[1+\lambda s(\mathbf{r})^2]), \tag{5}$$

where $\varepsilon_x^{\text{LDA}}$ and $\varepsilon_c^{\text{LDA}}$ are, respectively, the LDA exchange and correlation energy densities per electron, s is the reduced density gradient, $s=|\nabla\rho|/[2(3\pi^2)^{1/3}\rho^{4/3}]$, and $\lambda=0.8491/9=0.094\,34$.

The electron density $\rho(\mathbf{r})$ is expressed in terms of a Gaussian basis set $\{\chi_\mu(\mathbf{r})\}$ as

$$\rho(\mathbf{r}) = \sum_{\mu\nu} P_{\mu\nu}\chi_\mu(\mathbf{r})\chi_\nu(\mathbf{r}), \tag{6}$$

where $P_{\mu\nu}$ are the density matrix elements. For a self-consistent implementation of vdW-DF, we need to find the contribution of Eq. (2) to the Fock matrix. In other words, we need to evaluate the derivatives of E_c^{nl} with respect to $P_{\mu\nu}$. These derivatives are equal to the matrix elements of the corresponding correlation potential $v_c^{\text{nl}}(\mathbf{r})=\delta E_c^{\text{nl}}/\delta\rho(\mathbf{r})$,

$$\frac{dE_c^{\text{nl}}}{dP_{\mu\nu}} = \int d\mathbf{r}\chi_\mu(\mathbf{r})\frac{\delta E_c^{\text{nl}}}{\delta\rho(\mathbf{r})}\chi_\nu(\mathbf{r}) = \langle\mu|v_c^{\text{nl}}|\nu\rangle. \tag{7}$$

The nl correlation potential $v_c^{\text{nl}}(\mathbf{r})$ has been recently derived[17] and has the following form:

$$v_c^{\text{nl}}(\mathbf{r}) = \int d\mathbf{r}'\rho(\mathbf{r}')\phi(\mathbf{r},\mathbf{r}') + \int d\mathbf{r}'\rho(\mathbf{r}')\frac{\delta q_0(\mathbf{r}')}{\delta\rho(\mathbf{r})}\int d\mathbf{r}''\rho(\mathbf{r}'')\frac{\partial\phi}{\partial d}(\mathbf{r}',\mathbf{r}'')\times|\mathbf{r}'-\mathbf{r}''|. \tag{8}$$

To find the matrix elements of $v_c^{\text{nl}}(\mathbf{r})$, we can utilize the standard formalism[23] used with generalized gradient approximation (GGA) functionals,

$$\langle\mu|v_c^{\text{nl}}|\nu\rangle = \int d\mathbf{r}[F_\rho(\mathbf{r})\chi_\mu(\mathbf{r})\chi_\nu(\mathbf{r}) + 2F_\gamma(\mathbf{r})\nabla\rho(\mathbf{r})\nabla(\chi_\mu(\mathbf{r})\chi_\nu(\mathbf{r}))], \tag{9}$$

where

$$F_\rho(\mathbf{r}) = \frac{\partial q_0}{\partial\rho}(\mathbf{r})W(\mathbf{r}) + \int d\mathbf{r}'\rho(\mathbf{r}')\phi(\mathbf{r},\mathbf{r}'), \tag{10}$$

$$F_\gamma(\mathbf{r}) = \frac{\partial q_0}{\partial\gamma}(\mathbf{r})W(\mathbf{r}), \tag{11}$$

with

$$W(\mathbf{r}) = \frac{\rho(\mathbf{r})}{q_0(\mathbf{r})}\int d\mathbf{r}'\rho(\mathbf{r}')Q(\mathbf{r},\mathbf{r}'), \tag{12}$$

where we denoted

$$Q(\mathbf{r},\mathbf{r}') = d(\mathbf{r},\mathbf{r}')\frac{\partial\phi}{\partial d}(\mathbf{r},\mathbf{r}'). \tag{13}$$

The variable $\gamma=|\nabla\rho|^2$ is used for convenience of implementation. Partial derivatives $\partial q_0/\partial\rho$ and $\partial q_0/\partial\gamma$ are trivial since q_0 of Eq. (5) is a semilocal GGA functional.

The correlation kernel ϕ has a complicated form[14,17] involving a double integral that cannot be evaluated analytically. It is most efficient to precompute $\phi(d,d')$ numerically for a set of d and d' and compile a look-up table for use in the actual energy evaluations. The derivative $\partial\phi/\partial d$ can be found directly from the $\phi(d,d')$ look-up table via finite differences. This method is consistent with the bilinear interpolation we use to extract values from the $\phi(d,d')$ table. Note that our self-consistent implementation is somewhat simpler than the one described in Ref. 17 because in our code we do not need to evaluate the potential (8) at each grid point, but only need its matrix elements (9). In our code, only $\phi(d,d')$ is stored in the form of a numerical look-up table, whereas the method of Ref. 17 uses four look-up tables.

Within a Gaussian basis set implementation, the gradients of the total energy with respect to nuclear displacements contain not only the straightforward Hellman–Feynman terms but also the so-called "Pulay forces" arising due to the fact that the atom-centered basis functions as well as numerical quadrature grid points move together with the nuclei. E_c^{nl} contributes three terms to the Pulay forces,

$$\nabla_A E_c^{\text{nl}} = \mathbf{g}_{\text{GBF}}^A + \mathbf{g}_{\text{weights}}^A + \mathbf{g}_{\text{grid}}^A. \tag{14}$$

$\mathbf{g}_{\text{GBF}}^A$ refers to the contribution of the Gaussian basis functions. This term can be evaluated by plugging F_ρ and F_γ into

Eq. (9) of Ref. 23 instead of $\partial f/\partial\rho$ and $\partial f/\partial\gamma$.

The last two terms in Eq. (14) are due to the specific nature of our numerical quadrature integration technique. We employ the atomic partitioning scheme developed by Becke,[24] which separates the molecular integral into atomic contributions,

$$E_c^{\mathrm{nl}} = \frac{1}{2}\sum_A \sum_{i\in A} w_{Ai}\rho(\mathbf{r}_{Ai}) \sum_B \sum_{j\in B} w_{Bj}\rho(\mathbf{r}_{Bj})\phi(\mathbf{r}_{Ai},\mathbf{r}_{Bj}), \quad (15)$$

where w_{Ai} and w_{Bj} are the quadrature weights, and the grid points $\mathbf{r}_{Ai}$ are given by $\mathbf{r}_{Ai}=\mathbf{R}_A+\mathbf{r}_i$, where $\mathbf{R}_A$ is the position of nucleus A, with the $\mathbf{r}_i$ defining a one-center integration grid. The quadrature weights depend on the nuclear configuration and hence have a nonzero gradient with respect to nuclear displacements,

$$\mathbf{g}^A_{\mathrm{weights}} = \sum_B \sum_{i\in B} (\nabla_A w_{Bi})\rho(\mathbf{r}_{Bi}) \sum_C \sum_{j\in C} w_{Cj}\rho(\mathbf{r}_{Cj})\phi(\mathbf{r}_{Bi},\mathbf{r}_{Cj}). \quad (16)$$

The weight derivatives $\nabla_A w_{Bi}$ can be found in Ref. 23.

The last term in Eq. (14) arises because each one-center quadrature grid moves together with its parent nucleus and the nl correlation kernel ϕ depends explicitly on the distance between the grid points $r_{ij}=|\mathbf{r}_{Ai}-\mathbf{r}_{Bj}|$. The $\mathbf{g}^A_{\mathrm{grid}}$ term can be straightforwardly computed as

$$\mathbf{g}^A_{\mathrm{grid}} = \sum_{i\in A} w_{Ai}\rho(\mathbf{r}_{Ai}) \sum_{B\neq A} \sum_{j\in B} w_{Bj}\rho(\mathbf{r}_{Bj}) \frac{\partial\phi(\mathbf{r}_{Ai},\mathbf{r}_{Bj})}{\partial r_{ij}} \nabla_A r_{ij}, \quad (17)$$

with

$$\frac{\partial\phi(\mathbf{r}_{Ai},\mathbf{r}_{Bj})}{\partial r_{ij}} \nabla_A r_{ij} = [Q(\mathbf{r}_{Ai},\mathbf{r}_{Bj}) + Q(\mathbf{r}_{Bj},\mathbf{r}_{Ai})] \frac{\mathbf{r}_{Ai}-\mathbf{r}_{Bj}}{r_{ij}^2}. \quad (18)$$

Having implemented all the terms in Eq. (14), we compared our analytical gradients with numerical ones for several molecules and several choices of basis sets and quadrature grids. We find perfect agreement in each case.

Reference 14 defines the vdW-DF correlation functional leaving freedom of choice for the exchange component. It does not mean, however, that we can pair the vdW-DF correlation with any exchange functional. Care must be taken to avoid double counting. Semilocal exchange functionals that already predict binding or even overbinding in vdW complexes at short range are obviously not suitable to use with vdW-DF. Hartree–Fock (HF) exchange gives repulsive potential curves for vdW systems and can be paired with vdW-DF with moderate success.[15,16] The favorite choice of the developers of the vdW-DF functional[14] seems to be revPBE exchange.[25] In combination with vdW-DF correlation, revPBE was found to produce the most satisfactory results among semilocal GGA exchange functionals. In this work, besides HF and revPBE, we also consider another exchange functional: The long-range corrected LDA (i.e., Dirac/Slater) exchange, which we denote LCS. This functional is derived by splitting the Coulomb operator into short- and long-range parts with the help of the standard error function. The short-range (i.e., attenuated) LDA exchange[26,27] is then combined with the long-range HF exchange. Long-range corrected functionals, such as LCS, tend to give repulsive interactions in vdW complexes, just like HF does.[28] Such exchange functionals have been suggested as eminently suitable for adding a dispersion correlation term.[12,28–31] In LCS we use the range-separation parameter $\omega=0.5$ bohr^{-1}, which has been shown to work well in many cases.[32,33] LDA correlation, commonly used[32,33] alongside LCS exchange, is already a constituent of vdW-DF correlation of Eq. (1).

All the calculations reported in this paper have been performed self-consistently in a locally modified version of the Q-CHEM 3.1 software package.[34]

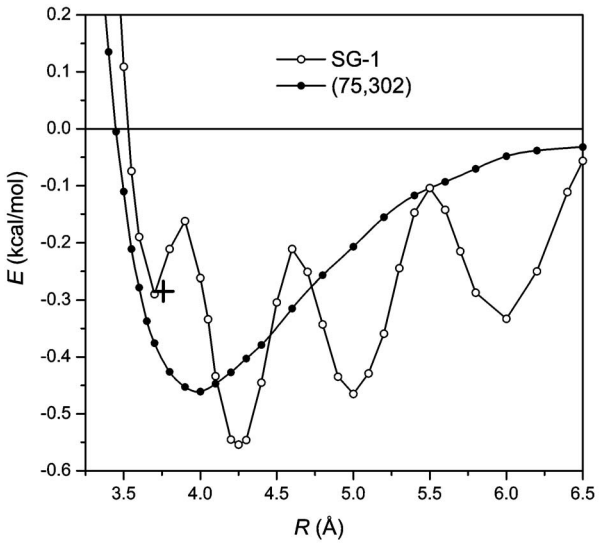

FIG. 1. Binding energy curves of Ar_2 computed with revPBE-vdW-DF and two different quadrature grids. Experimental equilibrium bond length and binding energy is marked by the "+" symbol. All calculations are self-consistent, using the aug-cc-pVTZ basis set.

III. TEST RESULTS

A. Numerical grid effects on the Ar_2 binding energy curve

To assess the sensitivity of the studied methods to the choice of the numerical integration grid, we compute binding energy curves of the Ar dimer using two different one-center quadrature grids: The Euler–Maclaurin–Lebedev (EML) (75,302) grid, containing 75 radial shells with 302 angular points per shell, and the standard SG-1 grid, which was derived[35] by pruning the EML-(50,194) grid. Note that we discard the grid points in the outermost shells where the electron density is negligibly small. After this additional pruning, the SG-1 scheme assigns approximately 2700 grid points per each Ar atom, and EML (75,302) uses about 17 000 points per Ar.

As shown in Fig. 1, revPBE-vdW-DF (that is revPBE exchange with vdW-DF correlation) with the EML-(75,302) grid yields a smooth binding energy curve similar to the one reported in Ref. 17 for the same system. However, if we use

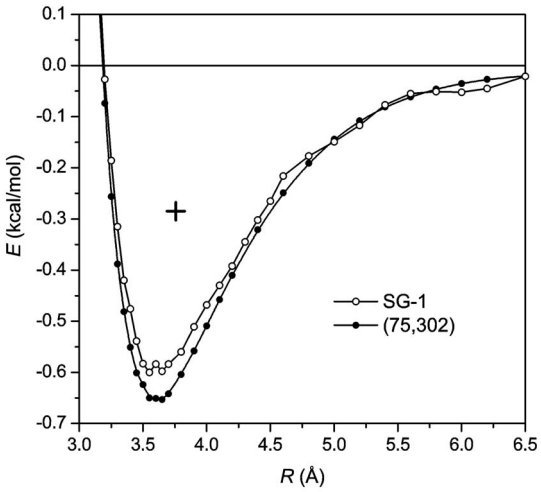

FIG. 2. The same as in Fig. 1 but computed with HF-vdW-DF.

the SG-1 grid, we observe large oscillations in the energy as a function of the internuclear distance R. Analysis of energetic contributions reveals that these oscillations arise almost entirely from the revPBE exchange.

In the case of HF-vdW-DF, the coarse SG-1 grid yields a binding energy curve that is reasonably close to the curve obtained with the finer (75,302) grid, as can be seen in Fig. 2. The HF-vdW-DF result with the SG-1 grid can be deemed acceptable since the numerical errors are much smaller than the inaccuracy of the method itself.

We have also computed the Ar_2 binding energy curve using LCS-vdW-DF and the SG-1 grid. We find an oscillatory dependence of the energy on R similar to the SG-1 curve in Fig. 1 for revPBE-vdW-DF. With the LCS exchange, oscillations are somewhat smaller in magnitude, although still unacceptable.

As far as the Ar_2 binding energy curve is concerned, we infer that the rather coarse SG-1 grid is sufficient for evaluating the vdW-DF correlation functional, but clearly insufficient for computing the contribution of semilocal exchange, such as revPBE, or even long-range corrected exchange, such as LCS. Hartree–Fock exchange is of course grid-free.

We note that an unpruned EML-type grid, such as (75,302), is wasteful since it uses unnecessarily too many grid points near nuclei. Unfortunately, there are no optimized pruned grids in Q-CHEM other than SG-1 and an even coarser SG-0. Hence, it may be advisable to develop a specialized pruned quadrature grid with better performance for weakly bound systems.

The computational cost for the nonlocal correlation functional scales quadratically with the number of grid points, whereas the cost of the semilocal part scales linearly. For optimal accuracy-to-cost ratio, it may seem natural to use a coarser grid (e.g., SG-1) for the nonlocal part and a finer (e.g., an unpruned EML) grid for the semilocal part. Such a solution, however, is not entirely satisfactory for technical reasons. The exchange-correlation contribution to the Fock matrix is evaluated by numerical integration of Eq. (9). The contributions from all semilocal and nonlocal parts of the functional can be integrated in a single step, provided that the same grid is used everywhere. Using different grids for different parts of the code would make a self-consistent implementation more cumbersome.

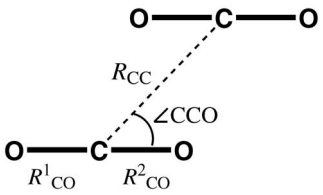

FIG. 3. Structural parameters of the CO_2 dimer.

B. CO_2 dimer

Accurate analytical gradients allow us to obtain equilibrium geometries of weakly bound systems without the need of computing binding energy curves. We have performed full geometry optimizations of the CO_2 dimer using several methods, with and without the nl dispersion correlation term. Experimental[36] and theoretical[37] studies show that the most stable structure of the dimer is slipped parallel configuration, i.e., planar with C_{2h} symmetry. Figure 3 shows this structure and defines structural parameters used in Tables I and II. All the methods listed in Tables I find an energetic minimum with such C_{2h} geometry. A part of the binding energy in the CO_2 dimer comes from the attractive interactions of the permanent quadrupole moments of the CO_2 monomers, so that some binding is predicted even without the nl vdW term. In Tables I and II, we included all combinations of three exchange functionals (revPBE, HF, and LCS) with two correlation functionals: The vdW-DF of Eq. (1) and just its local part in the VWN5 parametrization. As can be seen in Table I, inclusion of the dispersion term shortens the intermonomer separation and brings the CCO angle in a better agreement with experiment. Use of revPBE exchange results in longer R_{CC} distance as compared to HF or LCS.

Table I shows binding energies computed with and without counterpoise (CP) correction of the basis set superposition error (BSSE).[38] Since our "ghost atoms" contain quadrature grid points, the CP corrects not only BSSE but also the grid superposition error, which is non-negligible even with the EML-(75,302) grid. revPBE-vdW-DF yields a dissocia-

TABLE I. Binding energies and equilibrium structures of the CO_2 dimer, fully optimized in several methods. The aug-cc-pVQZ basis set and EML-(75,302) quadrature grid are used.

Method	D_e (kcal/mol) No CP	D_e (kcal/mol) CP	R_{CC} (Å)	∠CCO (deg)
revPBE-vdW-DF	1.79	1.50	3.81	57.5
HF-vdW-DF	3.17	2.86	3.36	57.7
LCS-vdW-DF	3.09	2.80	3.37	58.2
revPBE-VWN5	0.33	0.31	4.51	54.2
HF-VWN5	0.75	0.72	3.83	55.9
LCS-VWN5	0.61	0.59	3.92	55.5
Reference[a]	1.42		3.60	58.0

[a]D_e from Ref. 37 is the estimated CCSD(T) complete basis set limit. Experimental R_{CC} and ∠CCO are from Ref. 36.

TABLE II. The geometries of CO_2 monomers optimized individually and in a dimer. The aug-cc-pVQZ basis set and EML-(75,302) quadrature grid are used.

	Monomer	Dimer		
Method	R_{CO} (Å)	R^1_{CO} (Å)	R^2_{CO} (Å)	ΔE [a] (kcal/mol)
revPBE-vdW-DF	1.173	1.172	1.174	0.002
HF-vdW-DF	1.124	1.121	1.126	0.011
LCS-vdW-DF	1.144	1.142	1.146	0.011
revPBE-VWN5	1.175	1.174	1.175	0.001
HF-VWN5	1.124	1.123	1.125	0.006
LCS-VWN5	1.146	1.145	1.147	0.004
Expt.[b]	1.160			

[a]Monomer relaxation energy: $\Delta E = E(\text{unrelaxed } CO_2) - E(\text{relaxed } CO_2)$.
[b]r_e from Ref. 39.

tion energy in a reasonably good agreement with the reference value, whereas HF-vdW-DF and LCS-vdW-DF overbind by a factor of 2. Without the nl dispersion term, the dissociation energy is strongly underestimated, indicating that the interaction of permanent quadrupoles accounts only for a fraction of the total binding.

Binding energies in Table I were computed with respect to unrelaxed monomers. In other words, the energy of a CO_2 monomer was evaluated at the nuclear positions found in the dimer. In the optimized dimer structure, the two CO_2 moieties are perfectly linear but have slightly unequal CO bond lengths, as shown in Table II. For the sake of comparison, in Table II we also give the CO bond lengths in the individually optimized CO_2 molecules, as well as the experimental[39] CO_2 geometry. The monomer relaxation energy given in the last column of Table II shows that the dissociation energy of the CO_2 dimer will change only slightly if we compute it with respect to the optimized CO_2 moieties. Comparing the results obtained with vdW-DF versus VWN5 correlation in Table II, it can be clearly seen that the nl dispersion term has a very small effect on the covalent bond lengths. A similar observation was made in Ref. 17. As expected, the choice of the exchange component does affect the equilibrium bond lengths considerably: The CO bond is somewhat too short when HF exchange is used, but more accurate with revPBE or LCS.

In Ref. 17, the CO_2 dimer was studied with revPBE-vdW-DF. Unlike in the present work, a constrained optimization with rigid monomers was performed.[17] Nevertheless, the reported $R_{CC}=3.77$ Å, $\angle CCO=57.1°$, and $D_e=1.55$ kcal/mol are in good agreement with our results, shown in the first row of Table I.

C. Benzene-Ar complex

Another interesting test case for our implementation of vdW-DF is the benzene-Ar complex, which appears to be bound exclusively by dispersion interactions, just like the Ar dimer. Indeed, the local VWN5 correlation combined with either of the three exchange components yields a binding energy curve with only a barely noticeable minimum (about 0.05 kcal/mol in depth) at a large intermonomer distance ($R_{Ar}=5$ Å in revPBE-VWN5).

We have optimized the geometry of the benzene-Ar complex using vdW-DF with three choices of the exchange component. We report the equilibrium structural parameters in Table III. This complex has C_{6v} symmetry with Ar situated on the main symmetry axis. In Table III, R_{Ar} refers to the distance between the Ar atom and the plane drawn through the six C atoms.

For all three functionals given in Table III, we find that the geometry of the benzene ring in the benzene-Ar complex is almost completely unaffected by the presence of the Ar atom. Optimizing the geometry of the benzene molecule alone gives the same structure to within the numerical threshold. Experimental studies[42] of the benzene-Ar system seem to assume the rigidity of the benzene moiety. Our results confirm the validity of this assumption. The covalent bond lengths R_{CC} and R_{CH} are reasonably close to the experimental ones in all three methods. HF-vdW-DF is slightly worse than others with both CC and CH bonds a little too short.

As compared with experiment, the R_{Ar} distance is somewhat too long in revPBE-vdW-DF, but too short when HF or LCS exchange is used. Similar trends for intermonomer separations were observed for Ar_2 and $(CO_2)_2$ in previous sections.

In Table III we report binding energies computed with and without the CP correction. For the benzene-Ar system, the BSSE (which is the difference between "No CP" and "CP" values in Table III) in the aug-cc-pVTZ basis set is rather small on the scale of the total binding energy. All three methods overbind the complex, although overbinding is

TABLE III. Binding energies and equilibrium structures of the benzene-Ar complex, fully optimized in three different methods. The aug-cc-pVTZ basis set and EML-(75,302) quadrature grid are used.

	D_e (kcal/mol)		Distances (Å)		
Method	No CP	CP	R_{Ar}	R_{CC}	R_{CH}
revPBE-vdW-DF	1.42	1.38	3.74	1.402	1.088
HF-vdW-DF	2.52	2.41	3.36	1.364	1.061
LCS-vdW-DF	2.77	2.65	3.31	1.372	1.084
Expt.[a]	1.05		3.58	1.391	1.080

[a]D_0 from Ref. 40 corrected for zero-point energy from Ref. 41. R_{Ar} from Ref. 42. R_{CC} and R_{CH} from Ref. 43.

TABLE IV. Binding energies and equilibrium structures of the benzene-Ar complex, fully optimized with HF-vdW-DF in several basis sets. The SG-1 quadrature grid is used.

	D_e (kcal/mol)		Distances (Å)		
Method	No CP	CP	R_{Ar}	R_{CC}	R_{CH}
aug-cc-pVQZ	2.41	2.42	3.36	1.361	1.060
aug-cc-pVTZ	2.51	2.42	3.36	1.361	1.061
$6-311++G(3df,2p)$	2.71	2.47	3.31	1.361	1.061
$6-311++G(d,p)$	2.57	2.49	3.35	1.363	1.063

much more severe if HF or LCS exchange is used: The predicted dissociation energy is more than twice the experimental one.

Table IV shows the effects of the basis set size on the predictions of HF-vdW-DF for benzene-Ar. The SG-1 grid was used in this study. For HF-vdW-DF, the cheap SG-1 grid appears sufficient, as can be confirmed by comparing the aug-cc-pVTZ results from Table IV with the similar numbers in Table III obtained with a finer (75,302) grid. As Table IV demonstrates, the predicted equilibrium geometry of the benzene-Ar complex is not very sensitive to the choice of basis set, and the CP-corrected binding energy changes little from one basis set to another.

In Refs. 15 and 16, benzene dimers and monosubstituted benzene complexes were studied using the vdW-DF correlation functional with two choices of the exchange component: revPBE and HF. It was found that HF-vdW-DF overbinds these systems rather strongly and predicts somewhat too short intermonomer separations. revPBE-vdW-DF yields better binding energies but tends to give too long intermonomer separations. These trends are consistent with our findings for the test cases we used in this work. Note that despite considerable overbinding, HF-vdW-DF did a better job at predicting relative stability of different conformations of the complexes studied in Refs. 15 and 16, as compared to revPBE-vdW-DF.

IV. TIMING COMPARISONS

In a DFT calculation with a semilocal exchange-correlation functional and a good quality basis set, the most time-consuming part is typically the evaluation of the Coulomb energy (i.e., the mean-field Hartree term). Hybrid functionals introduce Hartree–Fock exchange, which becomes the most computationally expensive component. vdW-DF adds another time-consuming term, which is the nl correlation of Eq. (2). In this section, we compare the computational costs of these nonlocal energy components on the benchmark case of the benzene-Ar complex.

The DFT code in Q-CHEM currently does not make efficient use of molecular symmetry, so to compare the timings of different parts of the code on equal footing, we have completely disabled any use of symmetry by the program. To make our timings more consistent and reproducible, we also turned off the incremental Fock matrix algorithm, which speeds up Fock matrix calculation using information from previous iterations in the self-consistent field (SCF) procedure. We run our tests in parallel, in four threads, on an Intel Core-2 Quad node. Our benchmarking technique is by no means rigorous, so the timings given in Table V should be regarded only as rough order-of-magnitude comparisons for a typical execution environment.

The Fock matrix is usually evaluated simultaneously with the energy, and that is why they are grouped together in Table V. In the "Energy+Fock matrix time" column, we give the timing breakdown of one SCF cycle. In the last column of Table V we report the execution times needed for computing contributions to the gradients of the energy with respect to nuclear displacements.

The first two rows of Table V show the times needed to evaluate the mean-field Coulomb energy and its derivatives in two different basis sets. The third and the fourth rows show how these execution times increase after adding the Hartree–Fock exchange term. Note that the HF exchange is computed alongside the Coulomb energy in the same subroutine, which is considerably faster than computing them separately. The last two rows of Table V give the execution times for the nl vdW-DF correlation energy with two different quadrature grids. It is not possible to clearly say which component is the slowest because the time required for evaluating the Coulomb energy and HF exchange depends strongly on the basis set. Likewise, the time for the vdW-DF correlation depends strongly on the choice of the numerical grid. For each particular system of interest, one has to choose the computational details in such a way as to balance the desired accuracy with available computational resources. Let us reiterate, however, that the EML-(75,302) grid is wasteful and better optimized quadrature grids can lead to considerable time savings without loss of accuracy.

Comparison of the $E_c^{\text{vdW-DF}}$ timings in Table V obtained

TABLE V. Typical times (in seconds) required for computing the most time-consuming contributions to the energy, Fock matrix, and the gradient for the benzene-Ar complex without any use of molecular symmetry on an Intel Core-2 Quad node (see further details in the text).

Energy term	Computational details	Energy+Fock matrix time	Gradient time
Coulomb	$6-311++G(d,p)$	1	2
	aug-cc-pVTZ	25	50
Coulomb and HF exchange	$6-311++G(d,p)$	2	10
	aug-cc-pVTZ	120	700
$E_c^{\text{vdW-DF}}$	SG-1 grid	30	40
	EML-(75,302)	1100	1400

with two different quadrature grids reveals the steady quadratic scaling of the nl vdW-DF correlation with respect to the grid size. The EML-(75,302) grid uses about six times more grid points than SG-1; hence computing $E_c^{\mathrm{vdW-DF}}$ with EML-(75,302) is about 36 times slower than with SG-1. It is also obvious that, given a particular one-center quadrature grid, the vdW-DF correlation will exhibit a quadratic scaling with respect to the number of atoms in the system. Although vdW-DF is undeniably more expensive than semilocal or perhaps even hybrid functionals, it is computationally cheaper than most correlated wave function methods, which have less favorable scaling with the system size.

V. CONCLUSIONS

As evidenced by the number of interesting and useful computational studies published by the developers of vdW-DF to date,[14–21] the correlation functional introduced in Ref. 14 is a promising computational tool for weakly bound systems. In this paper we contribute to popularizing this method by showing how it can be efficiently and self-consistently implemented into a Gaussian basis based quantum chemistry software package. What makes our implementation even more useful is the availability of the accurate analytical gradients, which makes routine geometry optimizations possible.

We have tested the vdW-DF correlation functional in combination with three different exchange counterparts: Hartree–Fock exchange, a long-range corrected hybrid LCS, and a semilocal functional revPBE. All three of them, when used with no correlation, give repulsive interaction potentials for vdW complexes. However, pairing HF or LCS exchange with vdW-DF correlation results in considerable overbinding. vdW-DF gives satisfactory predictions of vdW binding energies only with revPBE exchange, which is the suggested choice of the vdW-DF developers.[14] revPBE exchange was originally intended[25] to be paired with PBE correlation[44] and its particular suitability for vdW-DF has not been adequately justified. So far, no other exchange approximation, besides revPBE, has been reported as a good match for vdW-DF correlation.

Among a few technical issues yet to be resolved in our code is the problem of the optimal choice of a quadrature grid. For acceptable numerical accuracy in calculations on weakly interacting systems, semilocal exchange functionals, such as revPBE, require rather fine grids, whereas for the nl correlation, a coarser grid is sufficient and desirable. Since evaluation of the Fock matrix is greatly simplified by using the same grid in all parts of the code, designing a grid adapted for this specific purpose may provide a compromise solution.

Hartree–Fock exchange is grid-free and, as implemented in Q-CHEM, relatively inexpensive. Therefore, for our purposes, HF would be a convenient starting point for designing nonlocal vdW functionals. As has been stated above, vdW-DF in its current version is not appropriately compatible with HF exchange.

ACKNOWLEDGMENTS

We acknowledge stimulating discussions with Timo Thonhauser. T.V. acknowledges a NSF CAREER Grant (Contract No. CHE-0547877) and a Packard Fellowship.

[1] A. J. Stone, *The Theory of Intermolecular Forces* (Clarendon, Oxford, 1996).
[2] A. Ruzsinszky, J. P. Perdew, and G. I. Csonka, J. Phys. Chem. A **109**, 11015 (2005), and references therein.
[3] Q. Wu and W. Yang, J. Chem. Phys. **116**, 515 (2002).
[4] S. Grimme, J. Comput. Chem. **25**, 1463 (2004).
[5] E. R. Johnson and A. D. Becke, J. Chem. Phys. **124**, 174104 (2006).
[6] P. Jurečka, J. Černý, P. Hobza, and D. R. Salahub, J. Comput. Chem. **28**, 555 (2007).
[7] Y. Andersson, D. C. Langreth, and B. I. Lundqvist, Phys. Rev. Lett. **76**, 102 (1996).
[8] J. F. Dobson and B. P. Dinte, Phys. Rev. Lett. **76**, 1780 (1996).
[9] W. Kohn, Y. Meir, and D. E. Makarov, Phys. Rev. Lett. **80**, 4153 (1998).
[10] A. J. Misquitta, B. Jeziorski, and K. Szalewicz, Phys. Rev. Lett. **91**, 033201 (2003).
[11] A. Heßelmann, G. Jansen, and M. Schütz, J. Chem. Phys. **122**, 014103 (2005).
[12] I. C. Gerber and J. G. Ángyán, J. Chem. Phys. **126**, 044103 (2007).
[13] J. Černý and P. Hobza, Phys. Chem. Chem. Phys. **9**, 5291 (2007).
[14] M. Dion, H. Rydberg, E. Schröder, D. C. Langreth, and B. I. Lundqvist, Phys. Rev. Lett. **92**, 246401 (2004); **95**, 109902(E) (2005).
[15] A. Puzder, M. Dion, and D. C. Langreth, J. Chem. Phys. **124**, 164105 (2006).
[16] T. Thonhauser, A. Puzder, and D. C. Langreth, J. Chem. Phys. **124**, 164106 (2006).
[17] T. Thonhauser, V. R. Cooper, S. Li, A. Puzder, P. Hyldgaard, and D. C. Langreth, Phys. Rev. B **76**, 125112 (2007).
[18] V. R. Cooper, T. Thonhauser, A. Puzder, E. Schröder, B. I. Lundqvist, and D. C. Langreth, J. Am. Chem. Soc. **130**, 1304 (2008).
[19] J. Kleis, B. I. Lundqvist, D. C. Langreth, and E. Schröder, Phys. Rev. B **76**, 100201 (2007).
[20] S. D. Chakarova-Käck, E. Schröder, B. I. Lundqvist, and D. C. Langreth, Phys. Rev. Lett. **96**, 146107 (2006).
[21] S. D. Chakarova-Käck, Ø. Borck, E. Schröder, and B. I. Lundqvist, Phys. Rev. B **74**, 155402 (2006).
[22] S. H. Vosko, L. Wilk, and M. Nusair, Can. J. Phys. **58**, 1200 (1980).
[23] B. G. Johnson, P. M. W. Gill, and J. A. Pople, J. Chem. Phys. **98**, 5612 (1993).
[24] A. D. Becke, J. Chem. Phys. **88**, 2547 (1988).
[25] Y. Zhang and W. Yang, Phys. Rev. Lett. **80**, 890 (1998).
[26] A. Savin, in *Recent Developments and Applications of Modern Density Functional Theory*, edited by J. M. Seminario (Elsevier, Amsterdam, 1996), pp. 327–357.
[27] P. M. W. Gill, R. D. Adamson, and J. A. Pople, Mol. Phys. **88**, 1005 (1996).
[28] M. Kamiya, T. Tsuneda, and K. Hirao, J. Chem. Phys. **117**, 6010 (2002).
[29] T. Sato, T. Tsuneda, and K. Hirao, J. Chem. Phys. **126**, 234114 (2007).
[30] J. G. Ángyán, I. C. Gerber, A. Savin, and J. Toulouse, Phys. Rev. A **72**, 012510 (2005).
[31] E. Goll, H.-J. Werner, and H. Stoll, Phys. Chem. Chem. Phys. **7**, 3917 (2005).
[32] I. C. Gerber and J. G. Ángyán, Chem. Phys. Lett. **415**, 100 (2005).
[33] O. A. Vydrov, J. Heyd, A. V. Krukau, and G. E. Scuseria, J. Chem. Phys. **125**, 074106 (2006).
[34] Y. Shao, L. Fusti-Molnar, Y. Jung, J. Kussmann, C. Ochsenfeld, S. T. Brown, A. T. B. Gilbert, L. V. Slipchenko, S. V. Levchenko, D. P. O'Neill, R. A. Distasio, Jr., R. C. Lochan, T. Wang, G. Jo. O. Beran, N. A. Besley, J. M. Herbert, C. Y. Lin, T. Van Voorhis, S. H. Chien, A. Sodt, R. P. Steele, V. A. Rassolov, P. E. Maslen, P. P. Korambath, R. D. Adamson, B. Austin, J. Baker, E. F. C. Byrd, H. Dachsel, R. J. Doerksen, A. Dreuw, B. D. Dunietz, A. D. Dutoi, T. R. Furlani, S. R. Gwaltney, A. Heyden, S. Hirata, C.-P. Hsu, G. Kedziora, R. Z. Khalliulin, P. Klunzinger, A. M. Lee, M. S. Lee, W. Liang, I. Lotan, N. Nair, B. Peters, E. I. Proynov, P. A. Pieniazek, Y. M. Rhee, J. Ritchie, E. Rosta, C. D. Sherrill,

A. C. Simmonett, J. E. Subotnik, H. L. Woodcock III, W. Zhang, A. T. Bell, A. K. Chakraborty, D. M. Chipman, F. J. Keil, A. Warshel, W. J. Hehre, H. F. Schaefer III, J. Kong, A. I. Krylov, P. M. W. Gill, and M. Head-Gordon, Phys. Chem. Chem. Phys. **8**, 3172 (2006).
[35] P. M. W. Gill, B. G. Johnson, and J. A. Pople, Chem. Phys. Lett. **209**, 506 (1993).
[36] M. A. Walsh, T. H. England, T. R. Dyke, and B. J. Howard, Chem. Phys. Lett. **142**, 265 (1987).
[37] S. Tsuzuki, T. Uchimaru, M. Mikami, and K. Tanabe, J. Chem. Phys. **109**, 2169 (1998).
[38] S. F. Boys and F. Bernardi, Mol. Phys. **19**, 553 (1970).
[39] G. Graner, C. Rossetti, and D. Bailly, Mol. Phys. **58**, 627 (1986).
[40] R. K. Sampson and W. D. Lawrance, Aust. J. Chem. **56**, 275 (2003).
[41] E. Riedle and A. van der Avoird, J. Chem. Phys. **104**, 882 (1996).
[42] Th. Weber, A. von Bargen, E. Riedle, and H. J. Neusser, J. Chem. Phys. **92**, 90 (1990).
[43] J. Gauss and J. F. Stanton, J. Phys. Chem. A **104**, 2865 (2000).
[44] J. P. Perdew, K. Burke, and M. Ernzerhof, Phys. Rev. Lett. **77**, 3865 (1996).